J Biol Phys (2006) 32:413–420
DOI 10.1007/s10867-006-9025-9

RESEARCH PAPER

Quantum Information Processing in the Wall of Cytoskeletal Microtubules

Chunhua Shi · Xijun Qiu · Tongcheng Wu · Ruxin Li

Received: 6 January 2006 / Accepted: 23 August 2006 /
Published online: 29 December 2006

Abstract Microtubules (MT) are composed of 13 protofilaments, each of which is a series of two-state tubulin dimers. In the MT wall, these dimers can be pictured as "lattice" sites similar to crystal lattices. Based on the pseudo-spin model, two different location states of the mobile electron in each dimer are proposed. Accordingly, the MT wall is described as an anisotropic two-dimensional (2D) pseudo-spin system considering a periodic triangular "lattice". Because three different "spin-spin" interactions in each cell exist periodically in the whole MT wall, the system may be shown to be an array of three types of two-pseudo-spin-state dimers. For the above-mentioned condition, the processing of quantum information is presented by using the scheme developed by Lloyd.

Key words MT · tubulin dimer · 2-D pseudo-spin · "lattice" site · two-state · information processing

1 Introduction

It is well-known that with the development of nanotechnology and the design of semiconductor and metal devices, the quantum size limit is being approached. Hence, the idea of quantum computers in which the elements that carry bits of information are atoms has attracted the attention of many scientists [1–7]. Generally, we assume that a minimal system for carrying a bit of information is a two-state atom. In fact, a computer is a set of elements, in which a bit of information can be transferred from one element to another, and each element should perform logical operations. Furthermore, it is possible in principle for a chain of two-state atoms to perform those logical operations [1, 2]. Therefore, quantum information can be represented by a set of two-state atoms.

C. Shi (✉) · X. Qiu · T. Wu
Department of Physics, Shanghai University, Shanghai 200444, People's Republic of China
e-mail: shi-chunhua@163.com

R. Li
Shanghai Institute of Optics and Fine Mechanics, Chinese Academy of Sciences,
Shanghai 201800, People's Republic of China

Table 1 Change of the initial states under the influence of the laser sequence

Initial states	$\omega_{01}^{A}\omega_{11}^{A}$	$\omega_{10}^{B}\omega_{11}^{B}$	$\omega_{01}^{A}\omega_{11}^{A}$
AB	AB	AB	AB
A*B	A*B	A*B*	AB*
AB*	A*B*	A*B	A*B
A*B*	AB*	AB*	A*B*

Asterisk means an atom is in the state $|1\rangle$.

In 1994, Lloyd [8] suggested a scheme of driving a quantum computer with a sequence of laser pulses, involving an array of weakly coupled atoms (nearest-neighbor interaction). Ref. [8] considered a one-dimensional (1D) array of two types ($AB\cdots$) of two-state atoms (either in the ground state $|0\rangle$, or in the excited state $|1\rangle$), in which each atom possesses a long-lived excited state and the resonant frequencies ω_A and ω_B. The appropriate laser pulses can transfer the atom from the state $|0\rangle$ to the state $|1\rangle$, or vice versa. However, different edge atoms can result in different information processing in the same pulse sequence due to the properties of the edge atoms. In Table 1, a laser sequence of the type $\omega_{01}^{A}\omega_{11}^{A}\omega_{10}^{B}\omega_{11}^{B}\omega_{01}^{A}\omega_{11}^{A}$ is used to move information along the above array. Noticeably, a laser pulse with the frequency of ω_{ij}^{K} (K represents A atom or B atom) only acts on the K atom, the left neighbor of which is in the state $|i\rangle$, and the right neighbor of which is in the state $|j\rangle$, and thus transfers the K atom from the state $|0\rangle$ to the state $|1\rangle$ or vice versa. As a result, there is an exchange of one information bit between the A and B atoms. In conclusion, by virtue of the edge atoms, using the appropriate sequence of laser pulses can complete the quantum information processing.

Recently, research on biological systems as important quantum information processors has attracted many physicists' interest [9]. Both experimental and theoretical work offers circumstantial evidence that non-trivial quantum mechanical processes might be at work in biological systems [9–14]. Penrose and Hameroff [13, 14] have proposed that MTs, important components and functional units in cytoskeletons as well as cellular organization and information processing, function as quantum computers. Consequently, the subject of information processing of MTs has started to be studied extensively.

As a first step in the direction of biophysical studies, Nogales and Downing [15, 16] have determined the structure of tubulin by electron crystallography. It is important to understand how tubulin molecules interact with each other as well as with a large number of other proteins and ligands. In further work, they extend their understanding of the structure and learn more about the processes that give tubulin its unique properties by developing instrumentation and technology [17–20].

From X-ray crystallography [21], we know that MTs are hollow cylindrical polymers of the protein tubulin which are 25 nm in outer diameter. The MT wall is comprised of 13 longitudinal protofilaments, each of which is a series of tubulin dimers (8×4×5 nm). Each dimer consists of two slightly different monomers known as α-tubulin and β-tubulin, is an oriented dipole (β plus, α minus), and has a net mobile electron due to an abundance of acidic amino acids. This electron can be localized either more toward the α-tubulin (the state $|\alpha\rangle$) or more toward the β-tubulin (the state $|\beta\rangle$). Interestingly, it has been shown that GTP-GDP hydrolysis releases approximately 0.42 eV/molecule [22] accompanied by a conformational change according to this unbound mobile electron's localization. Thus, each tubulin dimer only has two basic conformational states $|\alpha\rangle$ and $|\beta\rangle$; the quantum information may be transferred when two states change.

Actually, some models for the MT dynamics have been presented [23–28]. For the tubulin dimer dipoles in MTs, some authors [26] have taken the well-known double-well potential model, which is very successful in many fields [29, 30]. However, based on the quantum

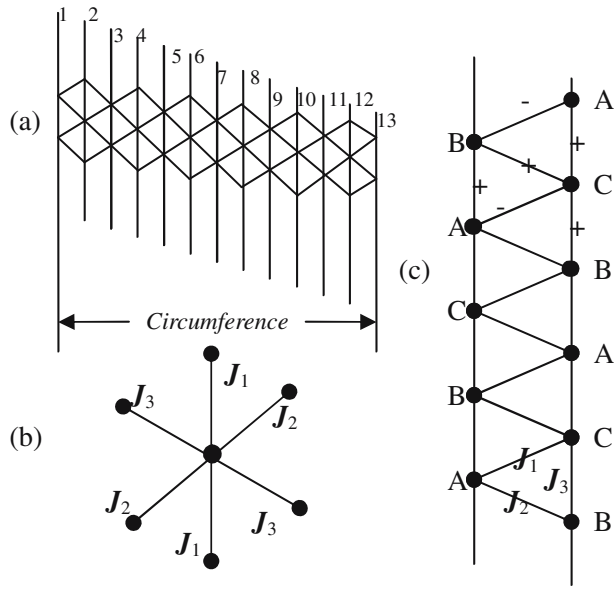

Fig. 1 (**a**) A band of triangles spanning the circumference of MT. (**b**) Exchange constants. (**c**) An array of three types of two-pseudo-spin-state dimers

character of the mobile electron and a matter worth noting: namely the fact that since quantum tunneling effects penetrate the barrier, each such double-well may be represented by one pseudo-spin [31]. In this work, the MT wall is described as an anisotropic 2D pseudo-spin system.

2 2D Pseudo-Spin System

The tubulin dimers within the MT wall are arranged in a "lattice" similar to the crystal lattice, which is slightly twisted, resulting in different neighbor relationships among each dimer and its six nearest neighbors [23]. This basic premise [23] physically views the entire MT as a regular array of coupled local dipole states, which interact with their immediate neighbors. Although the tubulin dimer undergoes two conformational changes, we adopt a simple "lattice" structure with the dimensions and orientations observed by X-ray crystallography of MTs [21]. In general, the MT wall can be described as a "lattice" with the minimal triangular periodic cell, and each dimer is regarded as a "lattice" site.

Considering the quantum characters of the mobile electron and the spin wave theory developed in solid state physics [32] and ferroelectrics, each such double-well may be replaced by one pseudo-spin. The two orientations (up $|0\rangle$ and down $|1\rangle$) of the pseudo-spin correspond to the two conformational states ($|\alpha\rangle$ and $|\beta\rangle$;) in the dimer. Using the pseudo-spin wave of the system, we can describe the distribution and the dynamic behavior of the mobile electrons. In this paper, a 1D pseudo-spin model [31] is straightforwardly extended to a 2D pseudo-spin model.

In the 2D pseudo-spin system, the Hamiltonian operator H may be divided into two parts: the one-body movement and the two-body electron-electron Coulomb interaction. The effective two-body interaction terms between neighboring "lattice" sites (Fig. 1) are:

$$H_{\text{int}}(i) = -\frac{1}{2}\sum_{j\neq i} J_{ij} S_i^Z S_j^Z \tag{1}$$

where the site i may be localized at any one protofilament dimer, while j is localized in the neighborhood of the site i. Exchange constants J_{ij} take the values $J_{CA} = J_1$, $J_{AB} = J_2$ and $J_{BC} = J_3$ (Fig. 1b and c), with

$$J_{ij} = -4v_{+-+-}(i,j), \tag{2}$$

$$v_{\lambda\nu\gamma\delta} \cong \int\int w_\lambda^*(x-i)w_v(x-i)\frac{e^2}{\varepsilon|x-x'|} \times w_\gamma^*(x'-j)w_\delta(x'-j)dxdx'. \tag{3}$$

Here, $v_{\lambda\nu\gamma\delta}(i,j)$ represents the coupling between the two dimers at the sites i and j, which depends on the distance between the two sites, as well as the quantum doublet states λ, ν, γ and δ (all of which take only two values, i.e., "+" or "–"). Additionally, $w_\lambda(\mathrm{x}-\mathrm{i})$ and $w_\lambda^*(\mathrm{x}-\mathrm{i})$ represent the Wannier function and its conjugate, respectively.

Taking two harmonic potentials to simulate the double-well potential mentioned above, and taking the exchange constants J_{CA} of the A dimer and C dimer as an example, then from Eq. 3, we have

$$v_{+-+-}(C,A) \cong \int\int \varphi_+^*(C)\varphi_-(C)\frac{e^2}{\varepsilon|\overrightarrow{x}_C - \overrightarrow{x}_A|} \times \varphi_+^*(A)\varphi_-(A)dx_C dx_A, \tag{4}$$

where

$$\begin{aligned} \varphi_+(A) &= \frac{1}{\sqrt{2}}(\varphi(\eta_A - a) + \varphi(\eta_A + a)), \\ \varphi_-(A) &= \frac{1}{\sqrt{2}}(\varphi(\eta_A - a) - \varphi(\eta_A + a)), \end{aligned} \tag{5}$$

and

$$\varphi(\eta_A) = \left(\frac{m\omega}{\hbar\pi}\right)^{1/4} e^{-\eta_A^2/2}. \tag{6}$$

Here, ω is the frequency of the ground state of the harmonic oscillation potential, m is the mass of the electron, and the dimensionless parameter $\eta_A = \sqrt{\frac{m\omega}{\hbar}}A$. The expressions of $\varphi_+(C)$ and $\varphi_-(C)$ are similar to those involving A. Then, using Eq. 2, we may approximately obtain the numerical results for the coupling constants J_1, J_2 and J_3:

$$J_1 = 0.1976/\varepsilon,\ J_2 = 0.0243/\varepsilon \,\text{and}\, J_3 = 0.1164/\varepsilon\ \text{eV}, \tag{7}$$

where the ε is the dielectric constant of the medium. We may take ε=10 as was done in the previous paper [31].

From the above model, we can see that the triangle may be regarded as the minimal cell in the periodic "lattice" of the MT wall, where there are three different "spin-spin" interactions resulting in three different coupling constants J. Because the J can take three different values, the periodic cell can be considered as involving three types of two-pseudo-spin-state dimers. Hence, the entire MT wall can be described as the array of three types of two-pseudo-spin-state dimer chain (Fig. 1c), where there are two longitudinal protofilaments within the MT wall.

3 Quantum Information Processing

The first question of quantum computation is the choice of an appropriate system that can be realized as an actual device. In this work, choosing a system with inequivalent effective

'spins', we design the quantum computation on an array of three types of two-pseudo-spin-state dimers by virtue of Lloyd's scheme for loading and processing the information.

Then, for the system of an array of three types of two-pseudo-spin-state dimers, the Hamiltonian is written as (let $\hbar$=1):

$$H = E_0 - \frac{1}{2}\sum_i \left(\Omega\sigma_i^x + J_{i,i+1}\sigma_i^z\sigma_{i+1}^z\right), \tag{8}$$

where the subscript i represents the A, B or the C dimer; $J_{i,i+1}$ is the exchange constant; and σ_i^x and σ_i^z are the x and z components of the Pauli operator, respectively. $\Omega \simeq E_- - E_+$ is the energy splitting of the doublet state, induced by the tunneling penetration effect of the electron; here "±" represent the pseudo-spin doublet states, "+"denotes down-state $|0\rangle$, while "–" denotes up-state $|1\rangle$. And $E_0 = \frac{1}{2}(E_- + E_+) \approx \omega$ is the ground state energy of the harmonic oscillator.

For B dimers, when some of them are in the state $|0\rangle$, one can express the energy for the system:

$$\overline{E}_0 = \langle AB_0C|H|AB_0C\rangle, \tag{9}$$

where $|B_0\rangle$ denotes the state $|0\rangle$ of B dimers, and the state $|A\rangle$ represents the possible state $|A_0\rangle$ (i.e., the state $|0\rangle$ of the A dimer) or $|A_1\rangle$ (i.e., the state $|1\rangle$ of the A dimer), and similarly, the $|C\rangle$ represents the $|C_0\rangle$ or $|C_1\rangle$. From Eq. 9, and the Hamiltonian (Eq. 8), we have

$$\overline{E}_0 = E_0 - \frac{1}{2}\left[J_{AB}(-1)^a + J_{BC}(-1)^c + J_{CA}(-1)^{a+c}\right], \tag{10}$$

where a takes the value zero if the state $|A\rangle$ takes $|A_0\rangle$ and a=1 if $|A\rangle = |A_1\rangle$; similarly, the value of c is determined by either $|C_0\rangle$ or $|C_1\rangle$. Then, when other B dimers are in the state $|1\rangle$, the corresponding energy $\overline{E}_1$ is:

$$\overline{E}_1 = E_0 - \frac{1}{2}\left[-J_{AB}(-1)^a - J_{BC}(-1)^c + J_{CA}(-1)^{a+c}\right]. \tag{11}$$

Consequently, the difference ΔE between the energies of these two states is:

$$\Delta E = \overline{E}_1 - \overline{E}_0 = J_{AB}(-1)^{\mathrm{a}} + J_{BC}(-1)^{\mathrm{c}}. \tag{12}$$

From the Hamiltonian (Eq. 8), one can see that the system has been considered to have only nearest-neighbor interactions, which shift the energy level of each dimer. Hence, the energy shift (E_0−ΔE) of the dimer is a function of the states of its neighbors. This means that each energy level will split into four levels. As a result, we find the following four resonant frequencies for the system, which correspond to the four resonant energies of the B dimers:

$$\omega^B = \begin{cases} \omega_{00}^B \to \omega + J_{AB} + J_{BC} \\ \omega_{01}^B \to \omega + J_{AB} - J_{BC} \\ \omega_{10}^B \to \omega - J_{AB} + J_{BC} \\ \omega_{11}^B \to \omega - J_{AB} - J_{BC} \end{cases}. \tag{13}$$

In the same way, the four frequencies of A and C dimers can be given as:

$$\omega^A = \begin{cases} \omega_{00}^A \to \omega + J_{CA} + J_{AB} \\ \omega_{01}^A \to \omega + J_{CA} - J_{AB} \\ \omega_{10}^A \to \omega - J_{CA} + J_{AB} \\ \omega_{11}^B \to \omega - J_{CA} - J_{AB} \end{cases}, \quad \omega^C = \begin{cases} \omega_{00}^C \to \omega + J_{BC} + J_{CA} \\ \omega_{01}^C \to \omega + J_{BC} - J_{CA} \\ \omega_{10}^C \to \omega - J_{BC} + J_{CA} \\ \omega_{11}^C \to \omega - J_{BC} - J_{CA} \end{cases}. \tag{14}$$

where $J_{CA} = J_1$, $J_{AB} = J_2$ and $J_{BC} = J_3$ (Fig. 1c).

From Eqs. 13 and 14, it is observed that the values of the resonant frequencies $\omega_{i,j}^K$ satisfy the following expression:

$$\omega_{00}^C \geq \omega_{i,j}^K \geq \omega_{11}^C.$$

Using the method proposed in Ref. [31], we can estimate the value of the harmonic oscillation frequency ω, i.e., $\omega \simeq 1.16 \times 10^{14}$Hz. Thus, by virtue of Eqs. 13, 14 and 7 with ε=10, all of the frequencies $\omega_{i,j}^K$ (i, j=0,1; K=A, B, C) can be given, and they satisfy

$$1.6 \times 10^{14} \geq \omega_{i,j}^k \geq 0.6 \times 10^{14}(\text{Hz}).$$

In addition, the excitation wavelengths lie in the infra-red domain: 11~31 μm.

Therefore, as long as the initial state of edge dimer is given, a sequence of laser pulses consisting of $\omega_{i,j}^K$ can be designed to perform information processing in the wall of MT.

4 Conclusions

In the wall of MT, due to the inherent symmetry structure of the tubulin dimer and the electric properties, a 2D pseudo-spin model is presented, in which the double wall potential has been used to represent each $\alpha\beta$-dimer. It is intended to describe the physical dynamics of the unbound mobile electron in each dimer of the MT wall.

The model that we propose for the information processing in MTs is based on Lloyd's generic ideas for two-level systems. The whole MT wall is treated as the chain of three types of two-pseudo-spin-state dimers. A set of appropriate resonant frequencies has been given. Therefore, it may be concluded that specific frequencies of laser pulse excitations can be applied in order to generate quantum information processing.

However, a primary technical problem in the operation of such information processing is the delivery of the proper sequence of accurate laser-pulses. Fortunately, in the fields of ultrasensitive spectroscopy, ultrastable lasers, ultrafast laser and nonlinear optics, the fruits of decades of developments are very notable; especially, in recent years, the explosion of the interconnect between these fields has opened remarkable and unexpected progress [33]. For the present, relating to the result given in Sect. 3, we expect to perform an experiment, in which the experimental set-up may be designed to consist of three main parts: (1) the laser-based precision spectroscopy system, including the mode-locked femtosecond frequency comb, and special nonlinear photonic crystal fibers which broaden the femtosecond laser frequency comb to more than an optical octave to realize a frequency chain that links the radio frequency; (2) the femtosecond pulse-shaping system, which includes the modulator for the amplitude and phase of the femtosecond laser pulse; and (3) the signal-information processing system, including an ultrasensitive photon-detector and monitor as well as the computer. Concerning the MT, it is better to put the MT under the

low temperature condition in order to reduce the thermal disturbance and to deal with the MT in vitro to avoid some complicated problems which arise from the living activity of specimens.

On the other hand, it is believed that there exist some kinds of coherent oscillations which arise from electric dipolar systems in living cells. In general, they possess frequencies over a wide range of 10^6–10^9 Hz [34] and 10^9–10^{11} Hz [35], and even higher. These coherent dipole-oscillation waves may properly organize the sequences of excitation pulses and may be applied along the length of MTs in order to carry on quantum information processing. In this context, we note that there is a particular model of MT information processing potential, which utilizes the Fröhlich excitations of tubulin subunits within MTs to support computation and information processing.

References

1. Toffoli, T.: Bicontinuous extensions of invertible combinatorial functions. Math. Syst. Theory **14**, 13–23 (1981)
2. Deutsch, D.: Quantum theory, the Church-Turing principle and the universal quantum computer. Proc. Roy. Soc. Lond. A **400**, 97–117 (1985)
3. Feynman, R.P.: Quantum mechanical computers. Opt. News **11**, 11–20 (1985)
4. Monroe, C., Meekhof, D.M., King, B.E., Itano, W.M., Wineland, D.J.: Demonstration of a fundamental quantum logic gate. Phys. Rev. Lett. **75**, 4714–4717 (1995)
5. Shahriar, M.S., Bowers, J.A., Demsky, B.: Cavity dark states for quantum computing. Opt. Commun. **195**, 411–417 (2001)
6. Beznosyuk, S.A.: Modern quantum theory and computer simulation in nanotechnologies: quantum topology approaches to kinematic and dynamic structures of self-assembling processes. Mater. Sci. Eng. C **19**, 369–372 (2002)
7. Medvedev, D.M., Dmitry, M., Goldfield, E.M.: An open MP/ MPI approach to the parallelization of iterative four-atom quantum mechanics. Comput. Phys. Commun. **166**, 94–108 (2005)
8. Lloyd, S.: A potentially realizable quantum computer. Science **261**, 1569–1571 (1993)
9. Davies, P.C.W.: Does quantum mechanics play a non-trivial role in life? Biosystems **78**, 69–79 (2004)
10. Patel, A.: Quantum algorithms and the genetic code. Pramana **56**, 367–381 (2001)
11. Bashford, J.D., Tsohantjis, I., Jarvis, P.D.: A supersymmetric model for the evolution of the genetic code. Biochemistry **95**, 987–992 (1998)
12. Silverman, G.J., Cary, S., Aguilar, S., Dwyer, D.: A B-cell superantigen induced persistent “hole” in the B-1 repertoire. J. Exp. Med. **192**, 87–98 (2000)
13. Hameroff, S.R., Penrose, R.: Conscious events as orchestrated space-time selections. J. Conscious. Stud. **3**, 36–53 (1996)
14. Woolf, N.J., Hameroff, S.R.: A quantum approach to visual consciousness. Trends Cogn. Sci. **5**, 472–478 (2001)
15. Nogales, E.S., Wolf, G., Downing, K.H.: Structure of the tubulin dimer by electron crystallography. Nature **391**, 199–203 (1998)
16. Nogales, E.S., Downing, K.H., Amos, L.A., Lowe, J.: Tubulin and FtsZ form a distinct family of GTPases. Nat. Struct. Biol. **5**, 451–458 (1998)
17. Nogales, E.S., Whittaker, M., Milligan, R.A., Downing, K.H.: High-resolution model of the microtubule. Cell **96**, 79–88 (1999)
18. Löwe, J., Li, H., Downing, K.H., Nogales, E.: Refined structure of ab-tubulin at 3.5 Å. J. Mol. Biol. **313**, 1045–1057 (2001)
19. Hud, N.V., Downing, K.H.: Cryoelectron microscopy of l phage DNA condensates in vitreous ice: the fine structure of DNA toroids. Proc. Natl. Acad. Sci. U.S.A. **98**, 14925–14930 (2001)
20. Zhong, S., Dadarlat, V.M., Glaeser, R.M., Head-Gordon, T., Downing, K.H.: Modeling chemical bonding effects for protein electron crystallography: the transferable fragmental electrostatic potential (TFESP) method. Acta Cryst. A **58**, 162–170 (2002)
21. Amos, L.A., Klug, A.: Arrangement of subunits in flagellar microtubules. J. Cell Sci. **14**, 523–549 (1974)
22. Engelborghs, Y., Audenaert, A., Heremans, L., Heremans, K.: Secondary structure analysis of tubulin and microtubules with Raman spectroscopy. Biochim. Biophys. Acta **996**, 110–115 (1989)

23. Tuszynski, J.A., Hameroff, S.H., Sataric, M.V., Trpisova, B., Nip, M.L.A.: Ferroelectric behaviour in microtubule dipole lattices: implications for information processing, signalling and assembly/disassembly. J. Theor. Biol. **174**, 371–380 (1995)
24. Mavromatos, N.E., Nanopoulos, D.V.: On quantum mechanical aspects of microtubules. Int. J. Mod. Phys. B **12**, 517–542 (1998)
25. Mavromatos, N.E., Mershin, A., Nanopoulos, D.V.: QED-cavity model of microtubules implies dissipationless energy transfer and biological quantum teleportation. Int. J. Mod. Phys. B **16**, 3623–3642 (2002)
26. Satarć, M.V., Tuszyński, J.A., Žakula, R.B.: Kinklike excitations as an energy-transfer mechanism in microtubules. Phys. Rev. E **48**, 589–597 (1993)
27. Jibu, M., Hagan, S., Hameroff, S.R., Pribram, K.H., Yasue, K.: Quantum optical coherence in cytoskeletal microtubules: implications for brain function. Biosystems **32**, 195–209 (1994)
28. Chen, Y., Qiu, X.J.: Collective radiation of water in cyto skeletal microtubule. Acta Phys. Sin. **52**, 1554–1560 (2003)
29. Sataric, M.V., Koruga D., Ivic, Z., Zakula, R.: The detachment of dimers in the tube of microtubulin as a result of a solitonic mechanism. J. Mol. Electron. **6**, 63–69 (1990)
30. Collins, M.A., Blumen, A., Currie, J.F., Ross, J.: Dynamics of domain walls in ferrodistortive materials. I. Theory. Phys. Rev. B **19**, 3630–3644 (1979)
31. Chen, Y., Qiu, X.J., Dong, X.L.: A theory for cell microtubule wall in external field and pseudo–spin wave excitation. Physica, A (2006) (in press)
32. Haken, H.: Quantum Field Theory of Solids – An Introduction. North-Holland, New York (1976)
33. Hall, J.L., Ye, J., Diddams, S.A., Ma, L.-S., Cundiff, S. T., Jones D.J.: Ultrasensitive spectroscopy, the ultrastable lasers, the ultrafast lasers, and the seriously nonlinear fiber: a new alliance for physics and metrology. IEEE J. Quantum Electron. **37**, 1482–1492 (2001)
34. Pokorny, J., Jelnek, F., Trkal, V.: Electric field around microtubules. Bioelectroch. Bioener. **45**, 239–245 (1998)
35. Fröhlich, H.: Long-range coherence and energy storage in biological systems. Int. J. Quantum Chem. **2**, 641–649 (1968)